DATA ACQUISITION AND PROCESSING OF PARALLEL FREQUENCY SAR BASED ON COMPRESSIVE SENSING

Y. N. You, H. P. Xu*, C. S. Li, and L. Q. Zhang

School of Electronic and Information Engineering, Beihang University, Beijing, China

Abstract—Traditional synthetic aperture radar (SAR) utilizes Shannon-Nyquist theorem for high bandwidth signal sampling, which induces a complicated SAR system, and it is difficult to transmit and process a huge amount of data caused by high A/D rate. Compressive sensing (CS) indicates that the compressible signal using a few measurements can be reconstructed by solving a convex optimization problem. A novel SAR based on CS theory, named as parallel frequencies SAR (PFSAR), is proposed in this paper. PFSAR transmits a set of narrow bandwidth signals which compose the large total bandwidth. Therefore, PFSAR only uses much less data to obtain a superiority image compared with a traditional SAR system. The data acquisition mode of PFSAR is developed and an algorithm of target scene reconstruction based on compressive sensing applied to PFSAR is proposed. The azimuth imaging of PFSAR is carried out based on the Doppler Effect, and then, the range imaging is performed by using compressive sensing of parallel frequencies signal. Several simulations demonstrate the feasibility and superiority of PFSAR via compressive sensing.

1. INTRODUCTION

Synthetic aperture radar (SAR) [1] is an active detector with all-day and all-weather capability. Recently, ultra swath and high resolution are major requirements for SAR system. The traditional SAR system emits high bandwidth chirp signal to obtain high range resolution, which demands high sampling rate according to the Shannon-Nyquist theorem. Transmitting and processing the huge data generated by

high sampling is one of the main challenges of radar system design. Compressive sensing (CS) in [2] and [3] provides a novel method for sampling and recovering signals. It shows that a K-sparse signal (length of N) can be reconstructed using $O(K \log N)$ measurements with high probability. The dimension of measurements is obviously reduced compared with Nyquist sampling. The radar receiver based on CS is firstly presented in [4]. The CS radar receiver discards the pulse compression matched filter to simplify the radar system and absolutely decreases the A/D rate. In [5], high-resolution radar based on CS is proposed, and the CS radar employs a sufficiently "incoherent" pulse to reconstruct the observation scene. Pulse Doppler radar with compressive sampling [6] presents an approach to reduce the A/D sampling rate through importing complete sparse dictionaries and basis pursuit reconstruction algorithm. Radar signal processing based on CS efficiently overcomes the huge data in terms of the Shannon-Nyquist sampling. Then the complexity of system can be reduced with compressive sampling.

There are some researches about the application of CS to SAR. CS applied to compress SAR raw data is firstly proposed in [7]. It uses the dual tree complex wavelet transform for sparse decomposing of SAR image and the SAR raw signal is randomly sampled in two-dimensional (2D) fast Fourier transform (FFT) domain to achieve signal compression. [8] analyzes properties of SAR data and image and indicates that only the brightest objects of the SAR image are compressible. In [9, 10], Tello Alonso et al. propose a novel method for the focusing of raw data in radar imaging. Signal sampling and reconstruction based on CS is introduced as an alternative option to traditional matched filtering. In [11], white Gaussian matrix is used as a measurement matrix to detect the targets with one-dimensional (1D) signal and obtain 2D SAR images based on CS. Anitori et al. [12] use a stepped sequence of frequencies CS radar to illuminate the corner reflectors, and CS is applied with random selection of frequencies and angles. In [13], Dantzig selector via compressive sensing has been used to obtain a better radar imaging result than that of the conventional l_1-norm based on compressive sensing. The paper [14] overviews the use of sparse reconstruction and random projection approaches in radar imaging. The joint reconstruction method [15, 16] is introduced to obtain better phase information. In [17], based on the reflectivity kernel analysis of SAR original echoes, singular value decomposition-QR (SVD-QR) is used to select the subset of SAR echoes in both slow-time domain and fast-time domain. Xu et al. [18] discuss a new imaging modality based on Bayesian compressive sensing, and clutter is taken into consideration in this novel CS radar. In [19], the

proper sparse dictionary is used to represent the SAR complex echoes, and thus SAR imaging processing is a joint optimization problem for the magnitude and phase of the complex signals. [20] applies CS to linear array SAR and CS is used after the range matched filtering. [21] proposes a novel SAR imaging algorithm based on CS with multiple transmitters and multiple azimuth beams. [22] presents a 4-D SAR imaging scheme based on CS. In [23], Li et al. present some applications of compressed sensing for multiple transmitters multiple azimuth beams SAR imaging. [24] provides an algorithm of sparse reconstruction for SAR imaging based on compressed sensing. Linear array imaging method of traditional SAR by using compressive sensing is shown in [25].

Though the researches on compressive sensing applied to SAR system have certain achievements, there is no SAR system based on compressive sensing. The concept of parallel frequencies signal is firstly presented in [26] to explore the application of CS in pulse compression. The author assumes that some distinct frequencies are simultaneously transmitted and presents how to use these frequencies in parallel to achieve the pulse compression without the Doppler effect. We import the theory of parallel frequencies into SAR and propose a novel SAR imaging mechanism, i.e., Parallel Frequencies SAR (PFSAR). The PFSAR transmits parallel frequencies signal instead of chirp signal for 2D imaging. The azimuth imaging of PFSAR is carried out based on the Doppler effect and then the range imaging is performed by using compressive sensing. The data acquisition mode is developed in our research, in addition, an approach of signal processing via compressive sensing applied to PFSAR is discussed in this paper.

Section 2 reviews compressive sensing method. The structure of parallel frequency radar can be found in Section 3. Data acquisition and signal processing via compressive sensing are shown in Section 4. Targets are reconstructed by using priori phase information. In Section 5, compared with the conventional SAR images, the feasibility and the superiority of PFSAR via compressive sensing are confirmed by some simulations.

2. COMPRESSIVE SENSING METHOD

Assume that target scene $\mathbf{S}$ ($\mathbf{S} \in \mathbf{R}^N$) is sparse on a basis matrix $\mathbf{\Psi}_{N \times N}$ ($\Psi_{N \times N} = (\psi_1, \psi_2, \ldots, \psi_N)$). $\mathbf{S}$ is represented as

$$\mathbf{S} = \mathbf{\Psi}\mathbf{x}, \tag{1}$$

where $\mathbf{x}$ is a length of N sparse coefficient vector with K nonzero elements and K a measure of the sparsity of $\mathbf{x}$. In compressive sensing

method. $\mathbf{S}$ is measured through a linear projection onto a measurement matrix $\mathbf{\Phi}_{M \times N}$ (where $M \ll N$), the projection is presented in matrix notation as

$$\mathbf{y} = \mathbf{\Phi S} = \mathbf{\Phi \Psi x}, \tag{2}$$

where $\mathbf{y}$ is a measurement vector of length M.

The sparseness is the number of nonzero coefficients with a proper sparse basis. In practice, the compressed signal and sparse scene can be represented by a few large coefficients. It is very vital for the choice of sparse basis. For the first, in space domain, i.e., warship targets located on the sea background, thus it satisfies the conditions of sparse space. Secondly, for the complicated scene, it is not sparse in space domain, however, the echoes of the specific scene are sparse on a proper basis, for instance, chirplet basis, wavelet basis and so on. Therefore compressive sensing can achieve the applications of SAR with a proper sparse basis.

The dimension M of measurement $\mathbf{y}$ is much less than the dimension N of sparse coefficient vector $\mathbf{x}$. Therefore the Eq. (2) is an ill-posed problem. In other words, the problem is undetermined. By reason that vector $\mathbf{x}$ is compressible, the recovery of the sparse coefficient vector $\mathbf{x}$ from the measurement vector $\mathbf{y}$ is translated into solving a minimization of l_0 norm problem. In [3] and [27], several significant results concerning compressive sensing show that for the purpose of the convergent of reconstruction algorithm, namely, one K-sparse vector x can be exactly reconstructed by M measurements, recovery matrix $\mathbf{A} = \mathbf{\Phi \Psi}$ is required to satisfy Restricted Isometry Property (RIP). It is a significant consequence to ensure the convergence of the reconstruction algorithm and a detailed expression is given for it as follows,

$$1 - \delta \leq \frac{\|\mathbf{A x}\|_2}{\|\mathbf{x}\|_2} \leq 1 + \delta \quad (\delta > 0), \tag{3}$$

where δ is a minimal constant, $\| \cdot \|_2$ the l_2 norm, and $\mathbf{x}$ the sparse coefficient vector. The minimization of the l_0 problem shown is equivalent to the l_1 norm convex problem under the RIP condition. The convex problem is expressed as

$$\hat{\mathbf{x}} = \arg \min \{\|\mathbf{x}\|_1 : \mathbf{x} \in \mathbf{R}^N, \ \mathbf{y} = \mathbf{\Phi \Psi x}\}. \tag{4}$$

Convex problem is simplified to linear programming. Basis Pursuit (BP) and greedy algorithms in [28–30] such as Matching Pursuit (MP) and Orthogonal Matching Pursuit (OMP) [31] can effectively solve this problem, thus allowing reconstruction of sparse scene $\mathbf{S}$.
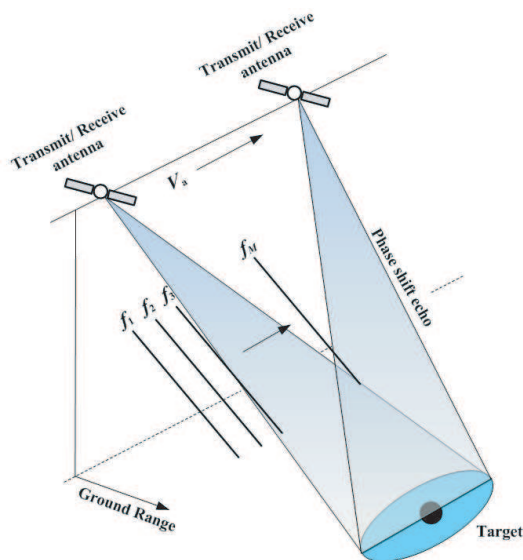
Figure 1. Observation mode of PFSAR.

3. PARALLEL FREQUENCY SAR

3.1. Observation Mode

The observation mode of PFSAR via compressive sensing is shown in Fig. 1. The radar platform moves along track (azimuth) direction with constant velocity, two-dimension observation scene is limited with the along track (azimuth) direction and the cross track (range) direction. The antenna pointing is vertical with azimuth direction, i.e., the beam direction is under zero squint case. PFSAR synchronously transmits M single frequency pulses with the constant step Δf in each azimuth, and then received the phase shift echoes. The total bandwidth can satisfy the requirements of high range resolution.

The beam footprint is divided into some equal observation cells, as shown in Fig. 2. The sparse targets will be located on the corresponding grid nodes. Location coordinate is Target (r, τ), r is range cell, τ is azimuth slow time, for instance, the location coordinate of the center point in Fig. 2(b) can be written as Target (r_c, τ_c). N_a and N_r respectively represents the sampling number of azimuth and range directions. The targets location information obviously depends on the observation grid.

Considering the movement of the radar platform along azimuth

(a)   (b)
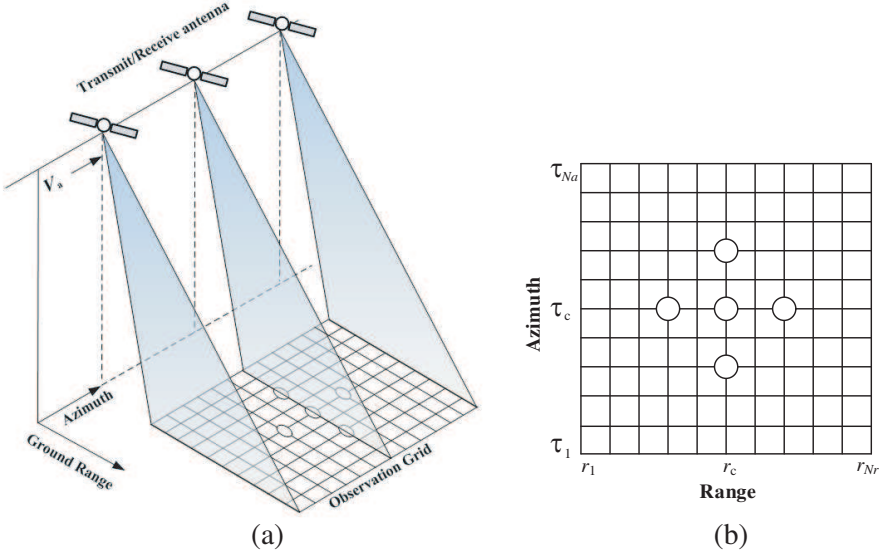
Figure 2. Observation grids of PFSAR via compressive sensing.

direction, the raw echo signal is written as

$$r(t,\tau) = Arect\left(t - \frac{2R(\tau)}{c}\right) A_a(\tau - \tau_c)e^{-j2\pi f_{\text{set}}\left(t - \frac{2R(\tau)}{c}\right)}, \quad (5)$$

where A is backscatter coefficient, *rect* the rectangle window, A_a the azimuth envelope, and c the light velocity. f_{set} is a set of transmitted frequencies, namely, $f_{\text{set}} = \{f_1, f_2, \ldots, f_M\}$. $R(\tau)$ is the instantaneous distance between the target and radar platform. According to the beam direction, we set the approximate representation $R(\tau) = R + V_a^2\tau^2/2R$ and R is the closest distance between the target and the radar platform.

3.2. Data Acquisition

PFSAR synchronously receives the phase shift echoes.   Fig. 3 demonstrates data acquisition process. Raw echoes are received by an antenna array, then the raw data are filtered through the multi-channel and the third step is quadrature demodulation. After demodulating, the intermediate frequency signals are sampled by a low-rate A/D converter, on condition that two-way I and Q mixing is employed in each channel, the sampling rate of A/D converter is effectively decreased into half.

Mixing and detecting phase is the most crucial processing stage, and the detail is depicted in Fig. 4. In view of several single frequency

Raw echo

Antenna array

Mixing and detecting phase

Multi-channel
filter

Quadrature
demodulation

Low-rate A/D

Complex data
memory

Download or Real-time processing
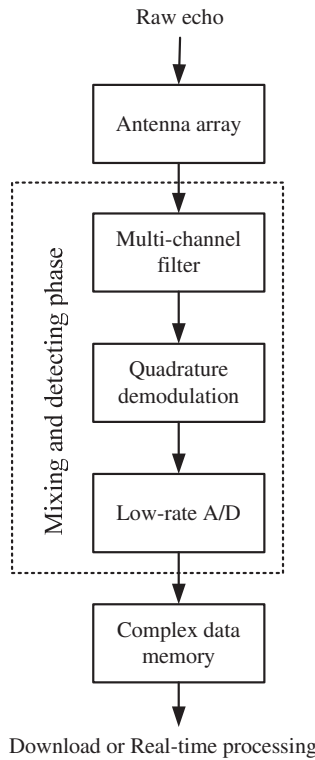
Figure 3. Data acquisition of PFSAR.

pulses congregating the raw echo, multi-channel filter is used to distinguish and extract the variously frequency pulses before mixing, through filtering procedure, the outputs of M channels is

$$\cos\left(2\pi f_1\left(t - \frac{2R(\tau)}{c}\right)\right), \quad \cos\left(2\pi f_2\left(t - \frac{2R(\tau)}{c}\right)\right), \ldots,$$
$$\cos\left(2\pi f_M\left(t - \frac{2R(\tau)}{c}\right)\right). \tag{6}$$

The output of each channel mixes with corresponding reference frequency, after mixing, the complex results composed with I and Q component are written as

$$\exp\left(j2\pi f_1\frac{2R(\tau)}{c}\right), \quad \exp\left(j2\pi f_2\frac{2R(\tau)}{c}\right), \ldots,$$
$$\exp\left(j2\pi f_M\frac{2R(\tau)}{c}\right). \tag{7}$$
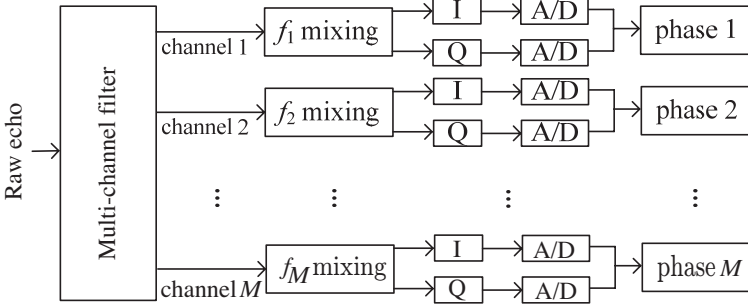
Figure 4. Mixing and detecting phases procedure.

The complex data as above are a set of phases containing range information of targets. In a certain azimuth time τ_i ($i = 1, 2, \ldots, N_a$), the complex data are written into a memory device in the channel sequence. Accordingly, memory space is three dimensional in mathematical expression, the first dimension is range cell, the second dimension is azimuth slow time, and the third dimension is the number of channels. In fact, the complex data can be written as one dimension data array, and each data cell needs to add the information about the azimuth slow time and the channels number, this additional information assists in resuming the raw complex data for imaging processing.

4. DATA PROCESSING BASED ON COMPRESSIVE SENSING

4.1. Azimuth Compressive

The processing of the backscattered signal is shown in Fig. 5. Through demodulating and detecting the phase shift, the echo signal can be written as

$$y_{\text{set}} = Ae^{-j2\pi f_{\text{set}} \frac{2R(\tau)}{c}} = Ae^{-j2\pi f_{\text{set}} \frac{2R}{c}} \cdot e^{-j2\pi f_{\text{set}} \frac{V_a^2 \tau^2}{cR}}. \tag{8}$$

Then we focus on the second exponent term in order to precisely draw the range information in the first exponent term. Obviously, the second exponent term is the result of the movement of the radar platform along azimuth direction and it has the feature of linear FM. Here, the FM rate is

$$K_a = 2V_a^2 / \lambda_{\text{set}} R. \tag{9}$$

The significant steps are K_a estimation and $\boldsymbol{\Phi}$ construction in imaging. Because of the second exponent in Eq. (8) varying with

Complex data
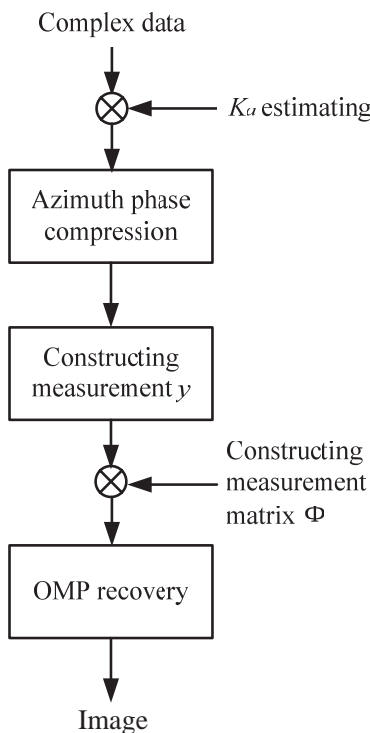
Figure 5. Two-dimensional signal imaging block diagram.

azimuth slow time, the targets will be focused on the respective zero Doppler by K_a before extracting the range information. K_a should be calculated precisely before compressing the azimuth phases. It also varies with the range cells and the signal frequencies. We use the autofocus to estimate the Doppler FM rate of the azimuth filter.

4.2. Range Processing via Compressive Sensing

Constructing the priori Φ is presented as follows. PFSAR transmits M single frequency pulses in a certain azimuth. The echo of the kth ($k = 1, 2, \ldots, M$) single frequency pulse is

$$r(t) = A rect\left(t - \frac{2R}{c}\right) e^{-j2\pi f_k\left(t - \frac{2R}{c}\right)}, \tag{10}$$

where c is the speed of light, A the backscatter coefficient of the target, f_k the frequency of the kth pulse, and $f_k = f_0 + k\Delta f \cdot f_0$ the carrier frequency. If we just collect the phase shift part the result is,

$$y_k = A e^{-j2\pi f_k \frac{2R}{c}}. \tag{11}$$

Let partition the maximum observation distance R_{MAX} into N points, thus the range cell is $\Delta R = R_{\text{MAX}}/N$. The discrete representation of Eq. (11) is written as

$$y_k = \sum_{n=0}^{N-1} e^{-j2\pi f_k \frac{2n\Delta R}{c}} \times A_n, \tag{12}$$

where A_n is the backscatter coefficient of the targets in the Nth point.

Aiming at an appointed observation scene, the targets locations are determined by the partition of observation grid. Supposing that there is a target in the center of the observation grid, the location coordinate is Target (r_c, τ_c) and the phase shift parts generated by target effecting under τ_c condition are

$$\exp\left(j2\pi f_1 \frac{2r_c}{c}\right), \ \exp\left(j2\pi f_2 \frac{2r_c}{c}\right), \ \ldots, \ \exp\left(j2\pi f_M \frac{2r_c}{c}\right). \tag{13}$$

Apparently, the targets in the observation grid with different locations still act on the transmitting signal that creates a set of fixed phases containing target range information. Provided each node has one target, we can utilize these fixed phases to construct the complete measurement matrix.

We write the Eq. (12) in matrix notation as

$$\mathbf{y} = \mathbf{\Phi S} = \mathbf{\Phi \Psi x}, \tag{14}$$

where $\mathbf{\Phi}$ is measurement matrix and

$$\mathbf{\Phi} = \{\phi_n\}_{n=0}^{N-1}, \tag{15}$$

where

$$\phi_n^T = \left\{e^{-j2\pi f_k \frac{2n\Delta R}{c}}\right\}_{k=1}^{M}. \tag{16}$$

$\mathbf{\Phi}$ accordingly contains the priori phases. The echoes in each azimuth slow time τ_i are linear combinations of random columns in the measurement matrix $\mathbf{\Phi}$. For fulfilling sparse scene condition, targets are much less than nodes in observation grid, then identity matrix $\mathbf{I}_{N \times N}$ is selected as the basis matrix. In that case, the recovery matrix $\mathbf{A}$ can be predigested as $\mathbf{\Phi \Psi} = \mathbf{\Phi I} = \mathbf{\Phi}$, thus the reconstruction algorithm merely uses $\mathbf{\Phi}$ as its recovery matrix.

OMP is employed as reconstruction algorithm. The input parameters of OMP are recovery matrix $\mathbf{A}$ and measurement set. In imaging system of parallel frequency radar, recovery matrix is the prior measurement matrix $\mathbf{\Phi}$ and the measurement set is the phase shift parts shown in Eq. (12). In addition, the output of OMP is the backscatter of targets, namely, the reconstruction result of Eq. (14) is the imaging of observation scene. The phase complex data are read as

the input of OMP in azimuth slow time τ_i sequence. This means the reconstruction result is the observation imaging of the corresponding azimuth slow time τ_i and the whole observation scene is composed of reconstruction results in each azimuth slow time.

In reconstruction algorithm, we also set some effective factors, for instance iterative times, error threshold and noise signal. High error threshold conduces more iterative times, and the imaging efficiency is degraded by the large computation load generated by each iteration. Noise signal also affects the success of reconstruction, so we compare the reconstructed results of noise free and noisy data in Section 5. In order to select the appropriate effecting factors in reconstruction algorithm, both imaging quality and algorithm efficiency should be taken into consideration.

5. SIMULATION RESULTS

5.1. Imaging with Noise-free Condition

Firstly, a single point is placed on the center observation node in the simulation. The parameters are selected as follows: $M = 30$, $\Delta f = 5\,\mathrm{MHz}$, $R_{\mathrm{MAX}} = 20\,\mathrm{km}$ and $N = 512$. Avoiding the influence of the different reconstruction algorithms, OMP is selected in the following simulations. Fig. 6 shows two-dimensional cross sections of a point target imaging.

As can be seen in Fig. 6, the side lobes of the range disappear via compressive sensing. Additionally, azimuth side lobes still exist and it has a significant impact on azimuth time information recovery if the
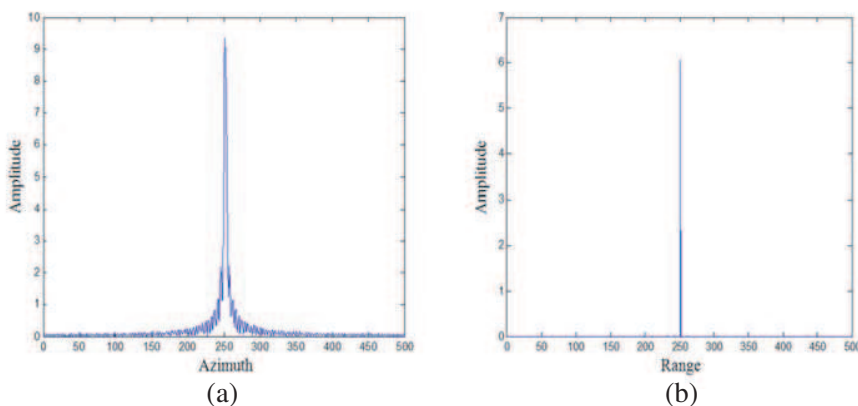
Figure 6. Point target cross sections of CS-based PFSAR. (a) Azimuth cross section. (b) Range cross section.

azimuth phases are not accurately focused.

The ability of distinguishing targets in the adjacent range cells visibly upgrades due to avoiding side lobes of the range. As shown in Fig. 7, three point targets with different backscatters are placed on the adjacent observation nodes along range direction. The inconspicuous backscatter point is completely submerged by the conspicuous point target in the imaging result of the traditional SAR. At the same time, the inconspicuous backscatter point is distinctly detected in the imaging result based on compressive sensing.

Figure 8 compares the several points two-dimensional imaging of PFSAR via compressive sensing with that of traditional SAR. The parameters represented in Table 1 are selected in the simulation.
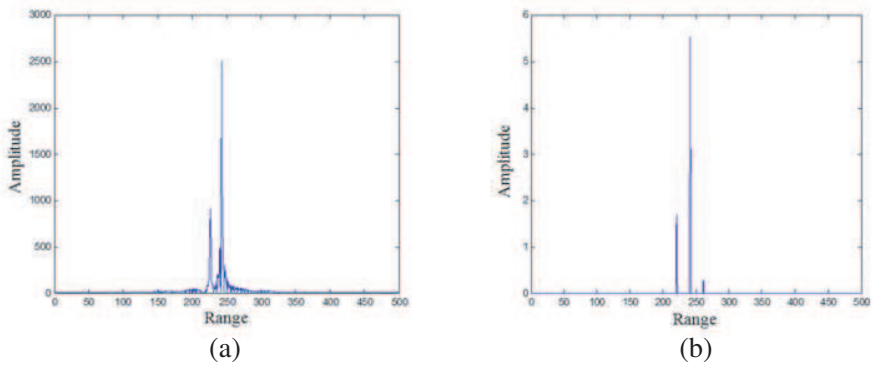
Figure 7. The ability of distinguishing the adjacent targets in the range direction with 3 point targets. (a) SAR. (b) CS-based PFSAR.
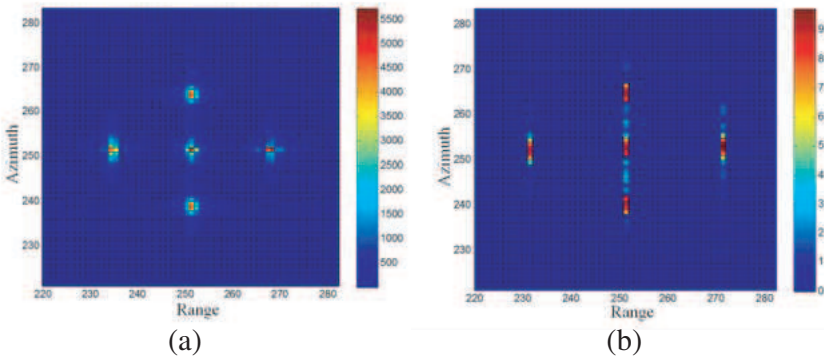
Figure 8. Imaging results of SAR and PFSAR via compressive sensing with several point targets. (a) SAR. (b) CS-based PFSAR.

Table 1. Simulation parameters in Fig. 8.

System bandwidth	30 MHz
Carrier frequency	1.5 GHz
Antenna length	10 m
Swath width	20 km
Pulse number	30
Pulse frequency step	1 MHz
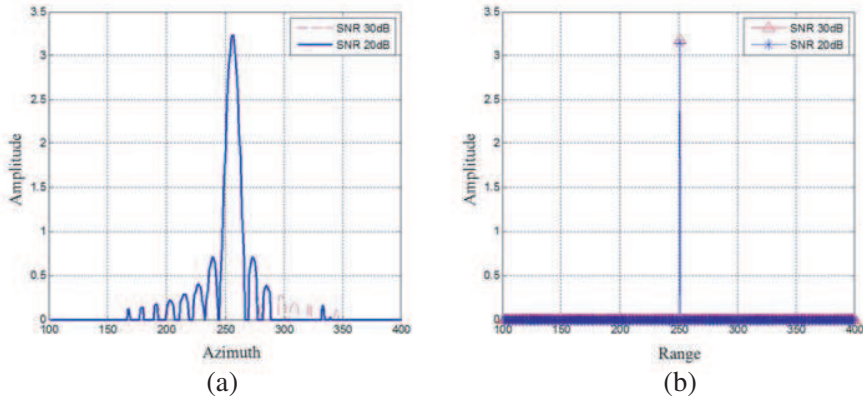
Figure 9. SNR 30 dB and SNR 20 dB. (a) Azimuth cross section. (b) Range cross section.
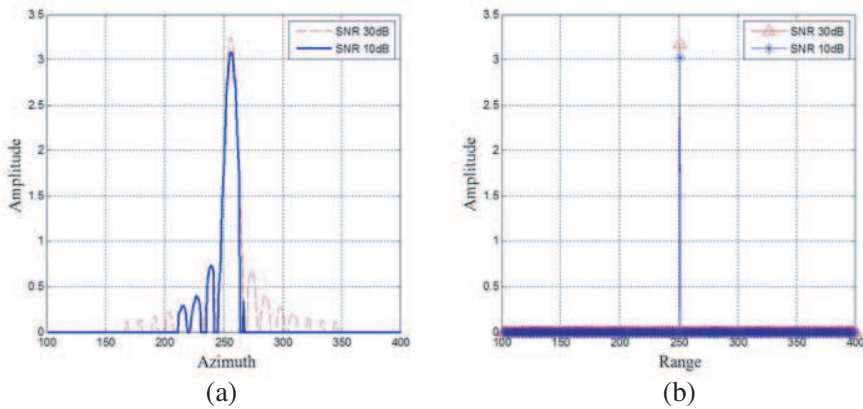
Figure 10. SNR 30 dB and SNR 10 dB. (a) Azimuth cross section. (b) Range cross section.
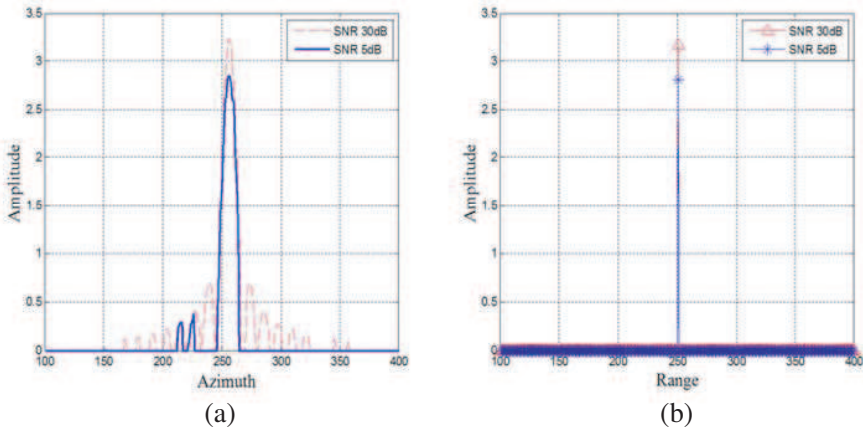
Figure 11. SNR 30 dB and SNR 5 dB. (a) Azimuth cross section. (b) Range cross section.

Different data amounts are used in this simulation, the data amount of PFSAR is 10% of the SAR data; however, PFSAR still shows evident superiority in range direction because of restraining side lobes of the range.

5.2. Imaging with Noise Interference

The noise in the received signal cannot be ignored in practice. More research is required on the capability of resisting the noise interference of the signal processing based on compressive sensing. The randomness of the noise makes the reconstruction results uncertain. The cross sections of the single point target with the different SNR are shown in Figs. 9, 10 and 11. Azimuth side lobes stochastically disappear with low SNR (20 dB, 10 dB and 5 dB). The backscatter of the single point target begins to decline from 10 dB SNR.

The sparsity of noise signal cannot achieve the same level of performance as the noise free signal with the constraint of l_2 norm. It is difficult to recover the accurate amplitude of the original signal, which is generally a characteristic of reconstructing noise signal by using compressive sensing, namely, amplitude loss.

6. CONCLUSION

This paper presents parallel frequency SAR and imaging approach based on compressive sensing. The novel radar can reduce data rate and maintain the large total bandwidth. The measurement

matrix $\boldsymbol{\Phi}$ is composed of the priori phases. The observation scene is reconstructed by OMP, and indeed this imaging approach avoids side lobes of the range. The recovery accuracy is improved according to information sampling via compressive sensing. It is confirmed by several simulations.

The noise interference is not ignored in the real radar system and then the echo of single point target is interfused with Gaussian random noise in correlative simulation. With the diminution of SNR, azimuth side lobes and the amplitude of backscatter begin to decline in imaging results. Amplitude loss appears in the reconstructed results.

Some of the ideas of further work are depicted finally. The scene complexity and measurement dimension also have an impact on reconstructed results. It is important to discuss if the range resolution can be improved through importing the complete partition of observation grid and prior range information of the targets.

REFERENCES

1. Chan, Y. K. and V. C. Koo, "An introduction to synthetic aperture radar (SAR)," *Progress In Electromagnetics Research B*, Vol. 2, 27–60, 2008.

2. Donoho, D., "Compressed sensing," *IEEE Transactions on Information Theory*, 4th edition, Vol. 52, 1289–1306, 2006.

3. Candes, E., "Compressive sampling," *Proceedings of the International Congress of Mathematicians*, 1433–1452, Madrid, Spain, 2006.

4. Baraniuk, R. and P. Steeghs, "Compressive radar imaging," *IEEE Radar Conference*, 128–133, April 2007.

5. Herman, M. A. and T. Strohmer, "High-resolution radar via compressed sensing," *IEEE Transactions on Signal Processing*, Vol. 57, 2275–2284, 2009.

6. Smith, G. E., T. Diethe, Z. Hussain, J. Shawe-Taylor, and D. R. Hardoon, "Compressed sampling for pulse Doppler radar," *IEEE Radar Conference*, 887–892, 2010.

7. Bhattacharya, S., T. Blumensath, B. Mulgrew, and M. Davies, "Fast encoding of synthetic aperture radar row data using compressed sensing," *IEEE Workshop on Statistical Signal Processing*, 448–452, Madison, USA, 2007.

8. Rilling, G., M. Davies, and B. Mulgrew, "Compressed sensing based compression of SAR raw data," *Signal Processing with Adaptive Sparse Structured Representations*, Saint-Malo(F), April 2009.

9. Tello Alonso, M., P. Lopez-Dekker, and J. Mallorqui, "A novel strategy for radar imaging based on compressive sensing," *IEEE International Geoscience and Remote Sensing Symposium*, Vol. 2, II-213–II-216, 2008.

10. Tello Alonso, M., P. Lopez-Dekker, and J. Mallorqui, "A novel strategy for radar imaging based on compressive sensing," *IEEE Transactions on Geoscience and Remote Sensing*, Vol. 48, No. 12, 4285–4295, 2010.

11. Lin, Y., Y. Wu, W. Hong, and B. Zhang, "Compressive sensing in radar imaging," *IET International Radar Conference*, 1–3, 2009.

12. Anitori, L, M. Otten, and P. Hoogeboom, "Compressive sensing for high resolution radar imaging," *Proceedings of Asia-Pacific Microwave Conference*, 1809–1812, 2010.

13. Mann, S., R. Phogat, and A. K. Mishra, "Dantzig selector based compressive sensing for radar image enhancement," *Annual IEEE India Conference, INDICON*, 1–4, 2010.

14. Potter, L. C., E. Ertin, J. T. Parker, and M. Cetin, "Sparsity and compressed sensing in radar imaging," *Proceedings of the IEEE*, Vol. 98, No. 6, 1006–1020, 2010.

15. Ramkrishnan, N., E. Ertin, and R. L. Moses, "Enhancement of coupled multichannel images using sparsity constraints," *IEEE Transactions on Image Processing*, Vol. 19, No. 8, 2115–2126, 2010.

16. Fornasier, M. and H. Rauhut, "Recovery algorithms for vector-valued data with joint sparsity constraints," *SIAM J. Numer. Anal*, Vol. 26, No. 2, 577–613, 2008.

17. Liang, Q., "Compressive sensing for synthetic aperture radar in fast-time and slow-time domains," *Proceedings of the IEEE*, 1479–1483, Asilomar, 2011.

18. Xu, J., Y. Pi, and Z. Cao, "Bayesian compressive sensing in synthetic aperture radar imaging," *IET Radar, Sonar and Navigation*, Vol. 6, No. 1, 2–8, 2012.

19. Samadi, S., M. Cetin, and M. A. Masnadi-Shirazi, "Sparse representation-based synthetic aperture radar imaging," *IET Radar, Sonar and Navigation*, Vol. 5, No. 2, 182–193, 2011.

20. Wei, S. J., X. L. Zhang, and J. Shi, "Linear array SAR imaging via compressed sensing," *Progress In Electromagnetics Research*, Vol. 117, 299–319, 2011.

21. Li, J., S. S. Zhang, and J. F. Chang, "Applications of compressed sensing for multiple transmitters multiple azimuth beams SAR imaging," *Progress In Electromagnetics Research*, Vol. 127, 259–

275, 2012.

22. Ren, X. Z., Y. F. Li, and R. L. Yang, "Four-dimensional SAR imaging scheme based on compressive sensing," *Progress In Electromagnetics Research B*, Vol. 39, 225–239, 2012.

23. Li, J., S. Zhang, and J. Chang, "Applications of compressed sensing for multiple transmitters multiple azimuth beams SAR imaging," *Progress In Electromagnetics Research*, Vol. 127, 259–275, 2012.

24. Wei, S.-J., X.-L. Zhang, J. Shi, and G. Xiang, "Sparse reconstruction for SAR imaging based on compressed sensing," *Progress In Electromagnetics Research*, Vol. 109, 63–81, 2010.

25. Wei, S.-J., X.-L. Zhang, and J. Shi, "Linear array SAR imaging via compressed sensing," *Progress In Electromagnetics Research*, Vol. 117, 299–319, 2011.

26. Ender, J. H. G., "On compressive sensing applied to radar," *Signal Processing*, Vol. 90, 1402–1414, 2010.

27. Candes, E., J. Romberg, and T. Tao, "Robust uncertainty principles: Exact signal reconstruction from highly incomplete frequency information," *IEEE Transactions on Information Theory*, Vol. 52, 489–509, 2006.

28. Blumensath, T. and M. Davies, "Gradient pursuits," *IEEE Transactions on Signal Processing*, Vol. 56, 2370–2382, 2008.

29. Davis, G., S. Mallat, and M. Avellaneda, "Greedy adaptive approximation," *Journal of Constructive Approximation*, Vol. 12, 57–98, 1997.

30. Donoho, D., M. Elad, and V. Temlyakov, "Stable recovery of sparse overcomplete representations in the presence of noise," *IEEE Transactions on Information Theory*, Vol. 52, 6–18, 2006.

31. Tropp, J. A. and A. C. Gilbert, "Signal recovery from random measurement via orthogonal matching pursuit," *IEEE Transactions on Information Theory*, Vol. 53, 4655–4666, 2007.